Original

Possible testosterone redundancy for 5α-dihydrotestosterone in the masculinization of mouse external genitalia

Yuko UEDA[1,2], Kentaro SUZUKI[2,3], Mizuki KAJIMOTO[2,4], Kota FUJIMOTO[2], Mala MAHENDROO[5], Masatsugu EMA[6], Gen YAMADA[2] and Isao HARA[1]

[1]*Department of Urology, Wakayama Medical University, 811-1 Kimiidera, Wakayama 641-0012, Japan*
[2]*Department of Developmental Genetics, Institute of Advanced Medicine, Wakayama Medical University, Wakayama 641-8509, Japan*
[3]*Faculty of Life and Environmental Sciences, University of Yamanashi, Yamanashi 400-0851, Japan*
[4]*Pharmacokinetics and Bioanalysis Center, Shin Nippon Biomedical Laboratories, Ltd. (SNBL), Kainan Intelligent Park, 16-1 Minami-Akasaka, Kainan, Wakayama 642-0017, Japan*
[5]*Department of Obstetrics and Gynecology, Green Center for Reproductive Biological Sciences, University of Texas Southwestern Medical Center, 5323 Harry Hines Blvd, Dallas, TX 75390-9032, USA*
[6]*Department of Stem Cells and Human Diseases Models, Research Center for Animal Life Science, Medical University of Shiga, Otsu, Shiga 520-2192, Japan*

Abstract: The development of embryonic external genitalia (eExG) into characteristic male structures, such as urethra and penile erectile tissues, depends on 5α-dihydrotestosterone (DHT). Although the corpus cavernosum (CC) is well known as essential for erectile function in adults, its developmental process and its dependency on DHT have been unknown. To reveal the dimorphic formation of the murine CC from the embryonic stage, we first analyzed the production of the protein vascular endothelial growth factor receptor-2 (FLK1) via its expression (hereinafter referred as "expression of FLK1") and the expression of alpha-smooth muscle actin (ACTA2) and collagen type 1 (COL1A1) in developing external genitalia. The 5-α reductase type 2 encoded by the SRD5A2 gene has been suggested to be a crucial enzyme for male sexual differentiation, as it converts testosterone (T) into DHT in the local urogenital organs. In fact, *SRD5A2* mutation results in decreased synthesis of DHT, which leads to various degrees of masculinized human external genitalia (ExG). We further investigated the expression profile of SRD5A2 during the formation of the murine CC. We observed that SRD5A2 was expressed in smooth muscle of the CC. To determine the role of SRD5A2 in CC formation, we analyzed the formation of erectile tissue in the male *Srd5a2* KO mice and measured the levels of androgens in the ExG by liquid chromatography-tandem mass spectrometry (LC-MS/MS). Intriguingly, there were no obvious defects in the CCs of male *Srd5a2* KO mice, possibly due to increased T levels. The current study suggests possible redundant functions of androgens in CC development.

Key words: 5α-dihydrotestosterone, 5-α reductase type 2, corpus cavernosum, external genitalia, redundancy

Introduction

External genitalia (ExG) are androgen-dependent organs showing prominently sexual differences. Exposure to androgens masculinizes the ExG, which is characterized as the formation of tubular urethra and corporal tissues. Development of the ExG starts from the common anlage, the genital tubercle (GT), in both males and fe-

males. In males, the GT differentiates into the penis under androgen actions. In females, the GT develops into the clitoris in the absence of androgen. Due to their sensitivity to androgen during ExG development, defective androgen production leads to congenital anomalies of ExG such as hypospadias and micropenis [1]. Although urethral tube formation has been well discussed, the development of the penile corpus cavernosum (hereafter referred to as the CC) is not understood. The CC is one of the major structures in ExG developing at the upper (dorsal) part of penis by androgen dependently [2]. It is known as the erectile tissue, which contains arterioles, sinusoidal spaces composed of endothelial cells, smooth muscle, and extracellular matrix (ECM) [3]. The sinusoidal spaces in the CC are essential structures for the influx of blood vessels during penile erection.

Testosterone (T) and 5α-dihydrotestosterone (DHT) are major androgens required for sexual differentiation of male reproductive organs. T is required for the development of Wolffian ducts and testis descent during the fetal period [4, 5] and the production of sperm in the seminiferous tubules [6, 7]. DHT is generally described as the more potent androgen and is required for the development of the ExG and prostate [8]. In humans, 5α-reductase type 2 deficiency (5α-SRD2) causes undermasculinized ExG, although it permits Wolffian duct development [9]. Thus, the androgen requirement for male sex differentiation is dependent on the types of organs.

Steroid 5α-reductase isozymes include three members (SRD5A1-3). SRD5A1 and 2 are mainly involved in the production of DHT from T. SRD5A3 is necessary for the conversion of polyprenol to dolichol, which is essential for N-linked protein glycosylation. *Srd5a3* knockout mice die in the early embryonic stage due to open neural tubes [10, 11]. In human, the 5-α reductase type 2 encoded by the SRD5A2 gene is a crucial enzyme for male sex differentiation by converting T into DHT in the ExG [12]. In mice, *Srd5a2* is expressed in the ventral side of the embryonic external genitalia (eExG) during urethral formation [13]. However, its expression pattern during ExG development has remained unknown [14].

In this study, we first performed SRD5A2 immunostaining analyses during CC formation. We subsequently performed a detailed histological analysis of the ExG of *Srd5a2* mutant mice. We discuss here the function of DHT in erectile tissue and a possible compensation of androgens for sexually dimorphic organ also by the measurement of local T and DHT levels by LC-MS/MS, which has higher sensitivity and specificity for steroid measurement [15, 16].

Materials and Methods

Animals

All procedures and protocols were approved by the Committee on Animal Research at Wakayama Medical University. *Srd5a1* KO mice, *Srd5a2* KO mice, and *Flk1-GFP* BAC Tg mice were utilized in this study [17–19]. *Srd5a1* and *Srd5a2* double knockout (*Srd5a1/2* DKO) mice were prepared by crossing males and females, which were heterozygous for type 1 and homozygous for the type 2 [18]. ICR and C57BL/6J mice were utilized as controls (CLEA Japan, Inc., Tokyo, Japan). Embryonic day 0.5 was defined as noon on the day when a vaginal plug was detected.

Histology and immunohistochemistry

ExGs were fixed overnight in 4% (wt/vol) paraformaldehyde (PFA) in phosphate-buffered saline (PBS) and dehydrated using methanol. Serial sections (6 μm) embedded in paraffin were prepared for hematoxylin/eosin staining and immunohistochemistry. For immunohistochemistry after deparaffinization and rehydration, the slides were subjected to antigen retrieval using citrate buffer (0.1 mM, pH 6.0) at 121°C for 1 min. For vascular endothelial growth factor receptor 2 (VEGFR2) staining, EDTA (0.1 mM, pH 8.0) was used as the antigen retrieval buffer. The following antibodies were used: anti-GFP antibodies (1:500, ab6556, Abcam, Cambridge, UK), anti-SRD5A2 antibodies (1:500, ab101896, Abcam), anti-ACTA2 antibodies (alpha-smooth muscle actin; 1:1,000, A2547, Sigma-Aldrich, St. Louis, MO, USA), anti-VEGFR2 antibodies (1:200, 2479 S, Cell Signaling, Danvers, MA, USA), and anti-AR antibodies (1:200, sc-815, Santa Cruz, Dallas, TX, USA).

Immunostaining was visualized by fluorescent staining (1/200, Alexa Fluor 488-conjugated IgG and an Alexa Fluor 546-conjugated IgG, Thermo Fisher Scientific, Waltham, MA, USA) and counterstained with Hoechst 33342 (1/1,000, Sigma-Aldrich). A Vector® TrueVIEW® Autofluorescence Quenching Kit (SP-8400, Vector Laboratories, Burlingame, CA, USA) was used to eliminate autofluorescence. For visualization of anti-VEGFR2 antibodies, immunocomplexes were detected with diaminobenzidine (DAB) staining. The tissue sections were counterstained with hematoxylin for 5 min. Images were acquired using a standard fluorescence microscope (BX51, Olympus®, Tokyo, Japan) and confocal microscopes (LSM 900, Zeiss®, Jena, Germany).

Direct androgen measurement by liquid chromatography–tandem mass spectrometry

For the measurement of androgen levels, male eExGs

were collected and immediately frozen in liquid nitrogen after dissection (n≥4). Testosterone and 5α-dihydrotestosterone levels were measured by liquid chromatography–tandem mass spectrometry (LC-MS/MS). The LC-MS/MS measurement protocol was performed as previously described [13].

Statistical analyses

All bar graphs show mean and SEM values. The statistical differences between groups were analyzed using Student's *t*-test followed by the *F*-test. A *P*-value of less than 0.05 was considered statically significant.

Results

Sexual dimorphism of CC formation during the development of murine external genitalia (ExG)

The location of major CC is in the proximal parts of the mouse ExG (Fig. 1A). The CC contains tunica albuginea at peripheral area (Figs. 1B and C; blue area) and sinusoidal spaces (Figs. 1B and C; green area) in mice ExG. To understand the formation of the CC, we performed histological analyses by HE staining. The CC was formed as mesenchymal condensations at dorsal (upper) site of urethra by embryonic day 18.5 (E18.5; Fig. 1D; yellow dotted line). At postnatal day 7 (PND7), sinusoidal spaces were formed (Fig. 1E; green dotted line) and a prospective tunica albuginea structure was observed in the outer region of the CC (Fig. 1E; blue

dotted line). Subsequently, the tunica albuginea thickened, and each sinusoidal space expanded adjacent to the tunica albuginea of the CC until PND21, which is considered the time of weaning and puberty in mice (Fig. 1F). In addition to the sinusoidal spaces and tunica albuginea, connective tissue developed at the center of the CC at PND21 (Fig. 1F; asterisk). These results indicate that the main components of CC development occurred prominently after birth. The CC was similar between male and female at E16.5. However, the size of CC showed sexual differences between males and females at E16.5 - PND21 (Supplementary Figs. 1A–J).

Next, we analyzed the expression of fetal liver kinase 1 (FLK1), alpha-smooth muscle actin (ACTA2), and collagen type I alpha chain (COL1A1) as markers for endothelium, smooth muscle, and collagen-containing cells, respectively. We utilized *Flk1-GFP* BAC transgenic mice to monitor the expression of FLK1 during CC development [19]. FLK1 was first expressed in both the male and female CC at E18.5 (Figs. 2A, B, F, and G). FLK1-positive cells were prominently increased in the outer region of the male CC after PND3 (Figs. 2C and D). Subsequently, the expression of FLK1 was maintained at PND21 (Fig. 2E). In the female CC, however, FLK- positive cells did not increase after birth (Figs. 2H–J).

The expression of ACTA2 was not detected in both male and female CC until E16.5 (Figs. 3A and F). In the male CC, ACTA2-positive cells were slightly observed
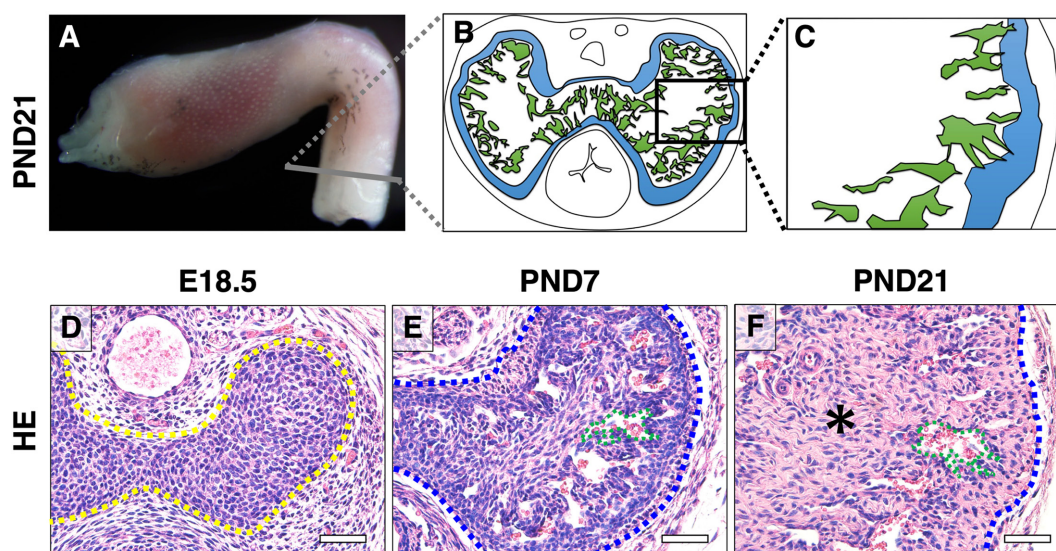

Fig. 1. The characteristic structure of the CC during external genitalia development. (A) Lateral whole-mount image of wild-type male mouse ExG at PND21. (B, C) A schematic illustration shows the highly magnified cross section at the gray line. The region in B enclosed in the black box. (D–F) Images of HE staining at E18.5, PND7, and PND21. The yellow dotted line indicates the CC. Blue dotted lines indicate the mouse tunica albuginea. Green dotted lines indicate the mouse sinusoidal space. The asterisk indicates connective tissue. CC, corpus cavernosum; ExG, external genitalia; HE, hematoxylin and eosin; E, embryonic; PND, postnatal day. Scale bar: 500 *μ*m.
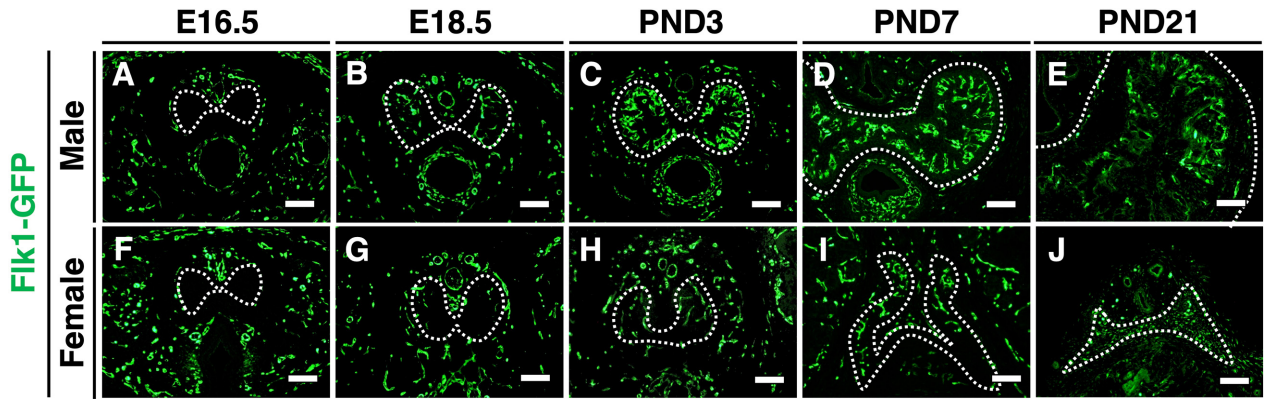
Fig. 2. Sexually dimorphic expression of FLK1 during CC development. (A–J) The expression of FLK1 in the male (upper panels) and female CCs (lower panels) at E16.5, E18.5, PND3, PND7, and PND21. In all immunofluorescent panels, Hoechst 33342 (blue) marks nuclei. White dotted lines indicate the outer region of the CC (tunica albuginea). Scale bar: 100 μm.
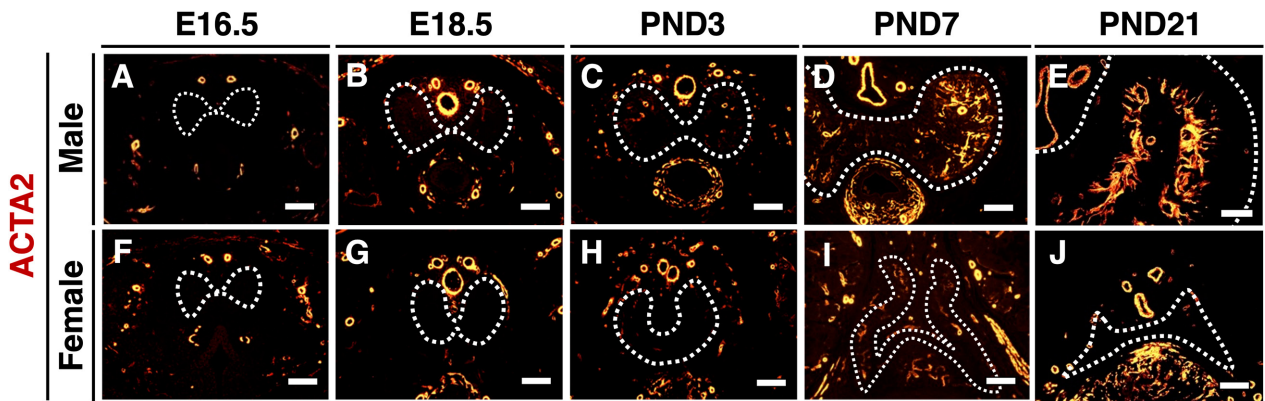

Fig. 3. Sexually dimorphic expression of ACTA2 during CC development. (A–J) The expression of ACTA2 in the male (upper panels) and female CCs (lower panels) at E16.5, E18.5, PND3, PND7, and PND21. White dotted lines indicate the outer region of the CC (tunica albuginea). Scale bar: 100 μm.
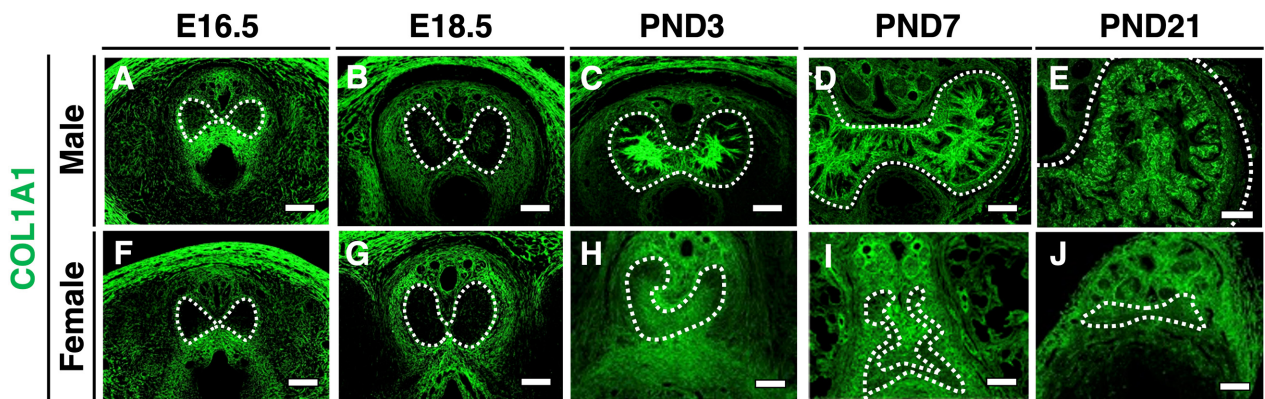

Fig. 4. Sexually dimorphic expression of COL1A1 during CC development. (A–J) The expression of COL1A1 in the male (upper panels) and female CCs (lower panels) at E16.5, E18.5, PND3, PND7, and PND21. White dotted lines indicate the outer region of the CC (tunica albuginea). Scale bar: 100 μm.

in the peripheral CC at E18.5 (Fig. 3B), and they were significantly increased after birth (Figs. 3C–E). In female CC, expression of ACTA2 was first observed at PND3 (Fig. 3H), which was later than in the male CC, but it did not increase thereafter (Figs. 3I and J).

The expression of COL1A1 was not detected in both male and female CC until E16.5 (Figs. 4A and F). In the male, COL1A1-positive cells were detected slightly in the center of the CC (Fig. 4B), and they gradually increased from PND3 to PND7 (Figs. 2C and D). Its ex-
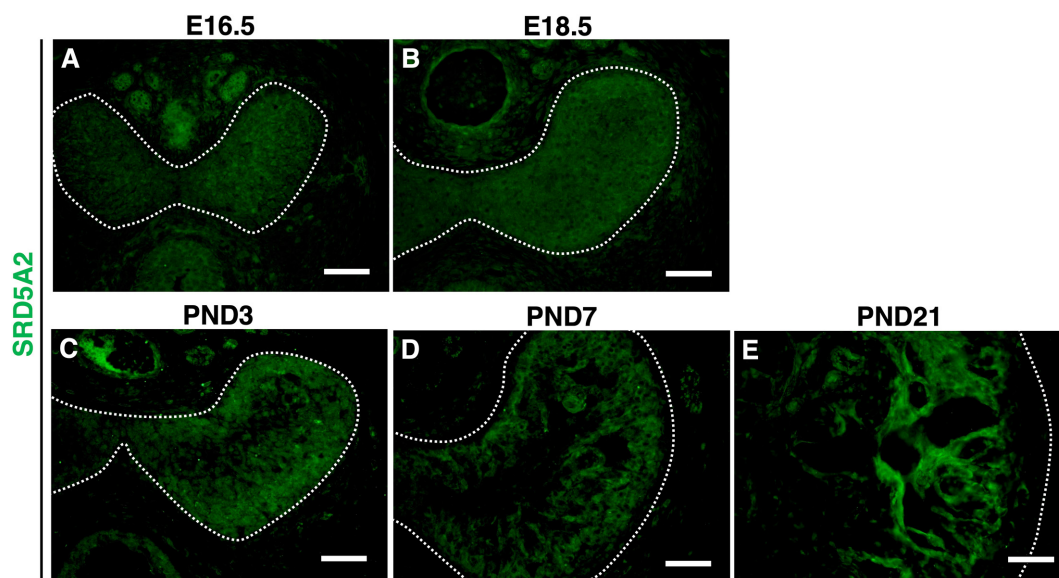
Fig. 5. The expression of SRD5A2 during CC development in male mice. (A–E) The expression of SRD5A2 at the embryonic stage and after birth. White dotted lines indicate the outer region of the CC (tunica albuginea). Scale bar: 500 μm.
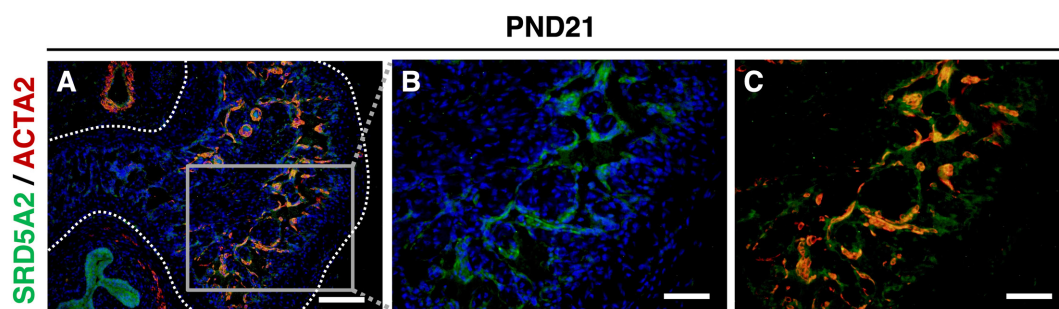

Fig. 6. The expression of SRD5A2 is localized with ACTA2-positive cells in the CC. (A–C) SRD5A2 is expressed with the smooth muscle marker ACTA2. White dotted lines indicate the outer region of CC (tunica albuginea). Scale bar: A, 250 μm; B–C, 500 μm.

pression was maintained at PND21 (Fig. 4E). In the female CC, COL1A1-positive cells were first observed at PND3 (Fig. 4H), which was later than in the male CC, and did not increase thereafter (Figs. 4I and J). These results suggest that the sexual dimorphism of CC formation occurs from the embryonic stages.

The expression of SRD5A2 in vascular smooth muscle cells of the CC at puberty

To get insights into SRD5A2 function during CC formation, we analyzed the profile of the expression of SRD5A2 by immunofluorescent (IF) staining by anti-SRD5A2 antibody. The expression of SRD5A2 was detected at the embryonic stage in the entire fetal CC (Figs. 5A and B), and then its expression became gradually more prominent in the peripheral region of CC after birth (Figs. 5C and D). At PND21, SRD5A2 appeared to be expressed in the surrounding sinusoidal spaces of the male CC (Fig. 5E). To further investigate where SRD5A2 was expressed in the CC, we performed co-immunofluorescent staining with anti-SRD5A2 and anti-ACTA2 antibodies at PND21. The expression of SRD5A2 was colocalized with ACTA2-positive cells, suggesting that it is expressed in vascular smooth muscle cells of the CC (Figs. 6A–C).

No obvious histological abnormalities in *Srd5a2* KO mice ExG

To determine the role of SRD5A2 in CC formation, we analyzed ExG of *Srd5a2* KO mice. There were no obvious defects in embryonic mutant mice (data not shown). Thus, we further investigated the adult male ExG of *Srd5a2* KO mice. *Srd5a2* KO male mice were morphologically similar with the control males at PND56 (Figs. 7A and B). The structures of the sinusoid, dorsal vein, and dorsal artery showed no obvious histological
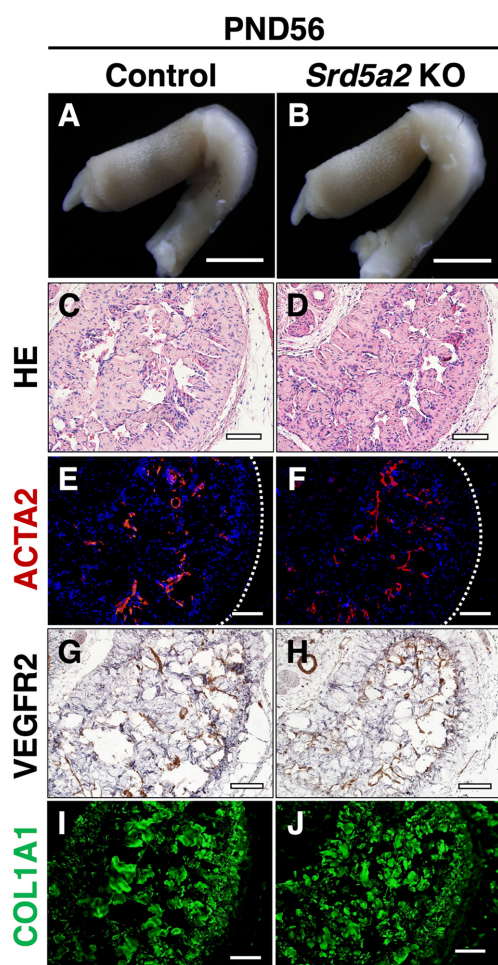
Fig. 7. Histological and immunofluorescence analysis of ExG between controls and *Srd5a2* KO mice. (A, B) Gross observation of ExG at PND56. (C, D) HE staining images for control and *Srd5a2* KO mice. (E–J) Immunofluorescence assays of the CCs of control and *Srd5a2* KO mice at PND56 with ACTA-2 antibody, VEGFR2, and COL1A1. White dotted lines indicate the outer region of the CC (tunica albuginea). Scale bar: 100 μm.

Fig. 8. Measurement of androgens in ExG and the expression of AR in *Srd5a2* KO mice. (A) Concentrations of DHT and (B) T in the CC of ExG at E17.5 measured by liquid chromatography-tandem mass spectrometry (LC-MS/MS). (C) Merged high-magnification images show the nuclear localization of AR in the control and *Srd5a2* KO mouse CC at PND56. AR is present in the nucleus in both the control and *Srd5a2* KO mouse sections. Scale bar in C: 100 μm. ExG, external genitalia; AR, androgen receptor; CC, corpus cavernosum; E, embryonic. Error bars represent the SEM. *$P<0.05$.

differences between controls and *Srd5a2* KO mice (Figs. 7A–D). Furthermore, the expression of ACTA2, VEGFR2 (a marker for endothelium), and COL1A1 in *Srd5a2* KO mice was not different compared with controls (Figs. 7E–J). To investigate possible compensatory functions of SRD5A1 in *Srd5a2* KO mice, we analyzed ExG of *Srd5a1/2* DKO mice. *Srd5a1/2* DKO mice showed no obvious abnormalities in ExG, suggesting that SRD5A1 did not play compensatory roles in *Srd5a2* KO mice (data not shown). These results suggest that masculinization of ExG occurs in *SRD5A2* KO mice while SRD5A2 is expressed during CC formation in normal mice.

Possible redundancy of local testosterone in eExG of *Srd5a2* KO mice

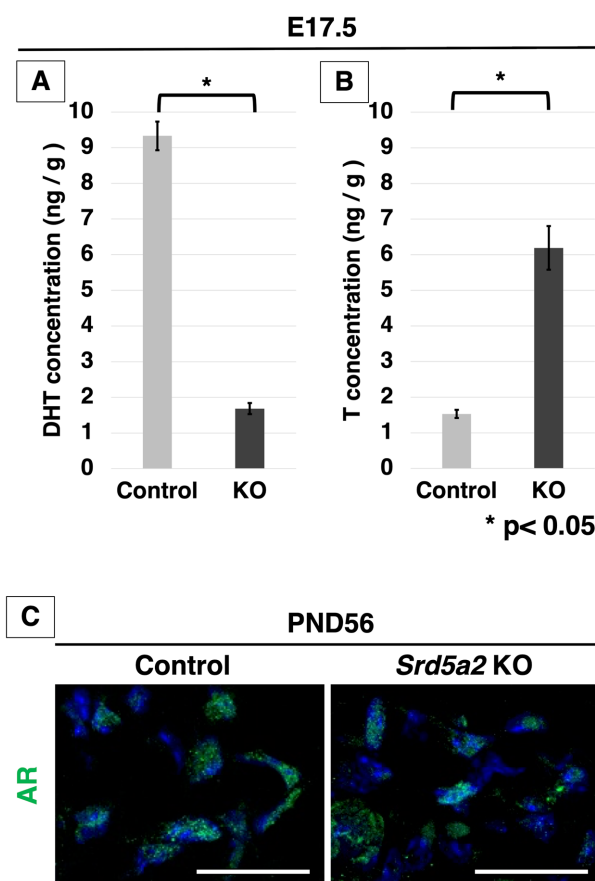To investigate a possible redundancy of testosterone (T) in loss of SRD5A2 function, we measured the local androgens (T and DHT) in male *Srd5a2* KO and control eExG at E17.5 using liquid chromatography-tandem mass spectrometry (LC-MS / MS). The level of DHT was significantly reduced in eExG of *Srd5a2* KO mice and was 18% of that of control (Fig. 8A). On the other hand, the T level was increased in eExG of *Srd5a2* KO mice (404% higher than that of control; Fig. 8B). These results suggest that redundantly increased T may masculinize mouse eExG instead of DHT.

Androgen receptor (AR) signaling is activated by binding androgen and translocating from the cytoplasm into the nuclei in external genitalia [20–22]. To confirm the activation of AR signaling in the CC of *Srd5a2* KO mice, we performed immunofluorescent staining with anti-AR antibodies. There were no obvious differences in its expression between *Srd5a2* KO male mice and the control at PND56 (Fig. 8C). AR was located in the nuclei

of sections from *Srd5a2* KO mice similarly with WT mice, indicating that AR signaling is activated in the CC of *Srd5a2* KO mice.

Discussion

The male corporal tissue, penile corpus cavernosum (CC) plays fundamental roles for erection. During erection, sinusoidal relaxation, arterial dilation, and venous compression occur [23]. Penile erection requires well-coordinated interactions between vascular endothelial cells (ECs), smooth muscle cells, and neuronal cells, and ECM [24]. Thus, defective formation and maintenance of the CC cause erectile dysfunction (ED) [25, 26]. Recently, its prevalence significantly increased with the aging populations and increased as lifestyle diseases [27–30]. Nevertheless, the developmental process of CC formation is still unknown. In the current study, we first revealed the onset of CC formation based on histological and immunohistological analyses. Endothelial cells, smooth muscle cells, and collagen deposition already started to develop in the late embryonic period and showed marked sex differences after birth. Intriguingly, such sex differences were observed in the late embryonic period. The current study is the first report for the developmental processes of the CC along with angiogenesis and collagen synthesis, which show sexual dimorphism.

Sexual dimorphism of the size of the ExG becomes significant after birth and is induced via the androgen-Wnt/β-catenin signaling pathway [2]. It has been reported that Dkk2, which encodes an extracellular antagonist of canonical Wnt/β-catenin signaling, is expressed dominantly in female CC compared with the male CC at E16.5, leading to sexually dimorphic activation of β-catenin signaling [2]. A previous paper suggests that endothelial β-catenin signaling is a promoting factor in angiogenesis [31]. In addition to being an angiogenic factor, it has been also reported that β-catenin is involved for collagen synthesis [32, 33]. Further analyses on Wnt/β-catenin signaling will reveal molecular mechanisms of CC formation under androgen signaling.

Androgens play an important role in maintaining the erectile tissue architecture, smooth muscle, endothelium, and connective tissue matrix [34]. The major circulating androgen, testosterone (T), is locally converted into 5a-dihydrotestosterone (DHT) by SRD5A2. In human, *SRD5A2* is expressed in the prostate, genital skin, epididymis, seminal vesicle, liver, and corpus cavernosum [35–38]. In this study, we observed that SRD5A2 was expressed in the CC from the embryonic to adult stages. Of note, SRD5A2 was expressed in smooth muscle cells surrounding sinusoids.

Regarding the possible interaction with DHT and paracrine factors for vascular cells, a recent study suggests that DHT can induce endothelial cell growth through a paracrine mechanism that is mainly mediated by VEGF in prostate cancer cells [39]. In addition to such a paracrine system, the autocrine and lumicrine manner of DHT and secreted factors may be essential regulator for the maintenance of reproductive organs [40]. SRD5A2 is expressed in vascular smooth muscle cells (VSMCs) isolated from the rat aorta and in both endothelial and smooth muscle cells of cerebral arteries [41, 42]. Further analysis will provide insights into the mechanisms of androgen-regulated angiogenesis in the CC.

Srd5a2 KO mice showed no obvious abnormalities in both embryonic and adult ExG. Although the local DHT level was dramatically reduced, the T level was increased in *Srd5a2* KO mice ExG compared with the controls. These results indicate whether a small amount of remnant DHT or redundantly increased T may be sufficient for masculinization of the mouse external genitalia. Androgens drive the development and maintenance of male characteristics by binding to androgen receptor (AR). DHT is generally considered to be more potent than T because it binds more tightly to AR [43]. It has also been reported to be approximately 10-fold more potent in the stimulation of AR target genes [44]. Kinetic experiments have shown that T at high concentrations interacts with AR similarly to DHT [45]. Thus, our data suggest that T may be redundant for DHT function in masculinization of the mouse external genitalia. The current study suggests the first functional redundancy effect of T on DHT in the reproductive organs.

There is a significant discrepancy between the current phenotypes in *Srd5a2* KO mice and symptoms in 5α-SRD2 patients. In human 5α-SRD2 patients, the phenotypic variability of genitalia ranges from perineal hypospadias, a clitoris-like phallus to an isolated micropenis [46]. Several publications have shown that some mutations of *SRD5A2* gene exons result in different phenotypes, but not all are correlated [9, 46–48]. *Srd5a2* KO mice did not show any obvious phenotypes due to the possible compensation via elevated T levels in local tissues. It has been discussed that T may accumulate in mouse ExG due to low levels of 17β-hydroxysteroid dehydrogenase enzyme activity, which converts T into less potent androgenic androstenedione in the dog prostate [18, 49–51]. Further analyses are necessary to investigate the possible differences in its enzymatic activity between species. Although there are phenotypic differences between mice and humans, the current mouse

model is expected to provide insight into the roles of androgen signals in local tissues.

References

1. Hiort O. The differential role of androgens in early human sex development. BMC Med. 2013; 11: 152. [Medline] [CrossRef]
2. Kajimoto M, Suzuki K, Ueda Y, Fujimoto K, Takeo T, Nakagata N, et al. Androgen/Wnt/beta-catenin signal axis augments cell proliferation of the mouse erectile tissue, corpus cavernosum. Congenit Anom (Kyoto). 2022.
3. Hashimoto D, Kajimoto M, Ueda Y, Hyuga T, Fujimoto K, Inoue S, et al. 3D reconstruction and histopathological analyses on murine corporal body. Reprod Med Biol. 2021; 20: 199–207. [Medline] [CrossRef]
4. Huhtaniemi I, Pelliniemi LJ. Fetal Leydig cells: cellular origin, morphology, life span, and special functional features. Proc Soc Exp Biol Med. 1992; 201: 125–140. [Medline] [CrossRef]
5. Miura K, Harikae K, Nakaguchi M, Imaimatsu K, Hiramatsu R, Tomita A, et al. Molecular and genetic characterization of partial masculinization in embryonic ovaries grafted into male nude mice. PLoS One. 2019; 14: e0212367. [Medline] [CrossRef]
6. Awoniyi CA, Santulli R, Sprando RL, Ewing LL, Zirkin BR. Restoration of advanced spermatogenic cells in the experimentally regressed rat testis: quantitative relationship to testosterone concentration within the testis. Endocrinology. 1989; 124: 1217–1223. [Medline] [CrossRef]
7. Matoba S, Ogura A. Generation of functional oocytes and spermatids from fetal primordial germ cells after ectopic transplantation in adult mice. Biol Reprod. 2011; 84: 631–638. [Medline] [CrossRef]
8. Swerdloff RS, Dudley RE, Page ST, Wang C, Salameh WA. Dihydrotestosterone: biochemistry, physiology, and clinical implications of elevated blood levels. Endocr Rev. 2017; 38: 220–254. [Medline] [CrossRef]
9. Cheng J, Lin R, Zhang W, Liu G, Sheng H, Li X, et al. Phenotype and molecular characteristics in 45 Chinese children with 5α-reductase type 2 deficiency from South China. Clin Endocrinol (Oxf). 2015; 83: 518–526. [Medline] [CrossRef]
10. Stiles AR, Russell DW. SRD5A3: A surprising role in glycosylation. Cell. 2010; 142: 196–198. [Medline] [CrossRef]
11. Mizuno S, Takami K, Daitoku Y, Tanimoto Y, Dinh TT, Mizuno-Iijima S, et al. Peri-implantation lethality in mice carrying megabase-scale deletion on 5qc3.3 is caused by Exoc1 null mutation. Sci Rep. 2015; 5: 13632. [Medline] [CrossRef]
12. Gad YZ, Nasr H, Mazen I, Salah N, el-Ridi R. 5 alpha-reductase deficiency in patients with micropenis. J Inherit Metab Dis. 1997; 20: 95–101. [Medline] [CrossRef]
13. Suzuki H, Matsushita S, Suzuki K, Yamada G. 5α-Dihydrotestosterone negatively regulates cell proliferation of the periurethral ventral mesenchyme during urethral tube formation in the murine male genital tubercle. Andrology. 2017; 5: 146–152. [Medline] [CrossRef]
14. Robitaille J, Langlois VS. Consequences of steroid-5α-reductase deficiency and inhibition in vertebrates. Gen Comp Endocrinol. 2020; 290: 113400. [Medline] [CrossRef]
15. Cao ZT, Botelho JC, Rej R, Vesper H. Accuracy-based proficiency testing for testosterone measurements with immunoassays and liquid chromatography-mass spectrometry. Clin Chim Acta. 2017; 469: 31–36. [Medline] [CrossRef]
16. de Oliveira LR, Longui CA, Guaragna-Filho G, da Costa JL, Lanaro R, Chiamolera MI, et al. Suggested cutoff point for testosterone by liquid chromatography with tandem mass spectrometry (LC-MS/MS) after stimulation with recombinant human chorionic gonadotropin. Sex Dev. 2021; 1–4. [Medline] [CrossRef]
17. Mahendroo MS, Cala KM, Russell DW. 5 alpha-reduced androgens play a key role in murine parturition. Mol Endocrinol. 1996; 10: 380–392. [Medline]
18. Mahendroo MS, Cala KM, Hess DL, Russell DW. Unexpected virilization in male mice lacking steroid 5 alpha-reductase enzymes. Endocrinology. 2001; 142: 4652–4662. [Medline] [CrossRef]
19. Ishitobi H, Matsumoto K, Azami T, Itoh F, Itoh S, Takahashi S, et al. Flk1-GFP BAC Tg mice: an animal model for the study of blood vessel development. Exp Anim. 2010; 59: 615–622. [Medline] [CrossRef]
20. Miyagawa S, Satoh Y, Haraguchi R, Suzuki K, Iguchi T, Taketo MM, et al. Genetic interactions of the androgen and Wnt/beta-catenin pathways for the masculinization of external genitalia. Mol Endocrinol. 2009; 23: 871–880. [Medline] [CrossRef]
21. Zheng Z, Armfield BA, Cohn MJ. Timing of androgen receptor disruption and estrogen exposure underlies a spectrum of congenital penile anomalies. Proc Natl Acad Sci USA. 2015; 112: E7194–E7203. [Medline] [CrossRef]
22. Kajioka D, Suzuki K, Matsushita S, Hino S, Sato T, Takada S, et al. Sexual fate of murine external genitalia development: Conserved transcriptional competency for male-biased genes in both sexes. Proc Natl Acad Sci USA. 2021; 118: e2024067118. [Medline] [CrossRef]
23. Dean RC, Lue TF. Physiology of penile erection and pathophysiology of erectile dysfunction. Urol Clin North Am. 2005; 32: 379–395. [Medline] [CrossRef]
24. Andersson KE. Mechanisms of penile erection and basis for pharmacological treatment of erectile dysfunction. Pharmacol Rev. 2011; 63: 811–859. [Medline] [CrossRef]
25. Zhang MG, Wang XJ, Shen ZJ, Gao PJ. Long-term oral administration of 5alpha-reductase inhibitor attenuates erectile function by inhibiting autophagy and promoting apoptosis of smooth muscle cells in corpus cavernosum of aged rats. Urology. 2013; 82: 743 e9–15.
26. Chen ZB, Li G, Lin H, Jiang J, Jiang R. Low androgen status inhibits erectile function by increasing pyroptosis in rat corpus cavernosum. Andrology. 2021; 9: 1264–1274. [Medline] [CrossRef]
27. Ayta IA, McKinlay JB, Krane RJ. The likely worldwide increase in erectile dysfunction between 1995 and 2025 and some possible policy consequences. BJU Int. 1999; 84: 50–56. [Medline] [CrossRef]
28. Johannes CB, Araujo AB, Feldman HA, Derby CA, Kleinman KP, McKinlay JB. Incidence of erectile dysfunction in men 40 to 69 years old: longitudinal results from the Massachusetts male aging study. J Urol. 2000; 163: 460–463. [Medline] [CrossRef]
29. Koskimäki J, Hakama M, Huhtala H, Tammela TL. Effect of

erectile dysfunction on frequency of intercourse: a population based prevalence study in Finland. J Urol. 2000; 164: 367–370. [Medline] [CrossRef]

30. Pallangyo P, Nicholaus P, Kisenge P, Mayala H, Swai N, Janabi M. A community-based study on prevalence and correlates of erectile dysfunction among Kinondoni District Residents, Dar Es Salaam, Tanzania. Reprod Health. 2016; 13: 140. [Medline] [CrossRef]

31. Martowicz A, Trusohamn M, Jensen N, Wisniewska-Kruk J, Corada M, Ning FC, et al. Endothelial β-catenin signaling supports postnatal brain and retinal angiogenesis by promoting sprouting, tip cell formation, and VEGFR (vascular endothelial growth factor receptor) 2 expression. Arterioscler Thromb Vasc Biol. 2019; 39: 2273–2288. [Medline] [CrossRef]

32. Cuevas CA, Gonzalez AA, Inestrosa NC, Vio CP, Prieto MC. Angiotensin II increases fibronectin and collagen I through the β-catenin-dependent signaling in mouse collecting duct cells. Am J Physiol Renal Physiol. 2015; 308: F358–F365. [Medline] [CrossRef]

33. Kholia S, Herrera Sanchez MB, Deregibus MC, Sassoè-Pognetto M, Camussi G, Brizzi MF. Human liver stem cell derived extracellular vesicles alleviate kidney fibrosis by interfering with the β-catenin pathway through miR29b. Int J Mol Sci. 2021; 22: 10780. [Medline] [CrossRef]

34. Traish AM. Androgens play a pivotal role in maintaining penile tissue architecture and erection: a review. J Androl. 2009; 30: 363–369. [Medline] [CrossRef]

35. Andersson S, Berman DM, Jenkins EP, Russell DW. Deletion of steroid 5 alpha-reductase 2 gene in male pseudohermaphroditism. Nature. 1991; 354: 159–161. [Medline] [CrossRef]

36. Eicheler W, Tuohimaa P, Vilja P, Adermann K, Forssmann WG, Aumüller G. Immunocytochemical localization of human 5 alpha-reductase 2 with polyclonal antibodies in androgen target and non-target human tissues. J Histochem Cytochem. 1994; 42: 667–675. [Medline] [CrossRef]

37. Levine AC, Wang JP, Ren M, Eliashvili E, Russell DW, Kirschenbaum A. Immunohistochemical localization of steroid 5 alpha-reductase 2 in the human male fetal reproductive tract and adult prostate. J Clin Endocrinol Metab. 1996; 81: 384–389. [Medline]

38. Kim KS, Liu W, Cunha GR, Russell DW, Huang H, Shapiro E, et al. Expression of the androgen receptor and 5 alpha-reductase type 2 in the developing human fetal penis and urethra. Cell Tissue Res. 2002; 307: 145–153. [Medline] [CrossRef]

39. Wen J, Zhao Y, Li J, Weng C, Cai J, Yang K, et al. Suppression of DHT-induced paracrine stimulation of endothelial cell growth by estrogens via prostate cancer cells. Prostate. 2013; 73: 1069–1081. [Medline] [CrossRef]

40. Kiyozumi D, Noda T, Yamaguchi R, Tobita T, Matsumura T, Shimada K, et al. NELL2-mediated lumicrine signaling through OVCH2 is required for male fertility. Science. 2020; 368: 1132–1135. [Medline] [CrossRef]

41. Fujimoto R, Morimoto I, Morita E, Sugimoto H, Ito Y, Eto S. Androgen receptors, 5 alpha-reductase activity and androgen-dependent proliferation of vascular smooth muscle cells. J Steroid Biochem Mol Biol. 1994; 50: 169–174. [Medline] [CrossRef]

42. Gonzales RJ, Ansar S, Duckles SP, Krause DN. Androgenic/estrogenic balance in the male rat cerebral circulation: metabolic enzymes and sex steroid receptors. J Cereb Blood Flow Metab. 2007; 27: 1841–1852. [Medline] [CrossRef]

43. Saartok T, Dahlberg E, Gustafsson JA. Relative binding affinity of anabolic-androgenic steroids: comparison of the binding to the androgen receptors in skeletal muscle and in prostate, as well as to sex hormone-binding globulin. Endocrinology. 1984; 114: 2100–2106. [Medline] [CrossRef]

44. Deslypere JP, Young M, Wilson JD, McPhaul MJ. Testosterone and 5α-dihydrotestosterone interact differently with the androgen receptor to enhance transcription of the MMTV-CAT reporter gene. Mol Cell Endocrinol. 1992; 88: 15–22. [Medline] [CrossRef]

45. Grino PB, Griffin JE, Wilson JD. Testosterone at high concentrations interacts with the human androgen receptor similarly to dihydrotestosterone. Endocrinology. 1990; 126: 1165–1172. [Medline] [CrossRef]

46. Maimoun L, Philibert P, Cammas B, Audran F, Bouchard P, Fenichel P, et al. Phenotypical, biological, and molecular heterogeneity of 5α-reductase deficiency: an extensive international experience of 55 patients. J Clin Endocrinol Metab. 2011; 96: 296–307. [Medline] [CrossRef]

47. Avendaño A, Paradisi I, Cammarata-Scalisi F, Callea M. 5-α-Reductase type 2 deficiency: is there a genotype-phenotype correlation? A review. Hormones (Athens). 2018; 17: 197–204. [Medline] [CrossRef]

48. Fan L, Song Y, Polak M, Li L, Ren X, Zhang B, et al. Clinical characteristics and genotype-phenotype correlations of 130 Chinese children in a high-homogeneity single-center cohort with 5α-reductase 2 deficiency. Mol Genet Genomic Med. 2020; 8: e1431. [Medline] [CrossRef]

49. Wenderoth UK, George FW, Wilson JD. The effect of a 5 alpha-reductase inhibitor on androgen-mediated growth of the dog prostate. Endocrinology. 1983; 113: 569–573. [Medline] [CrossRef]

50. Mustonen M, Poutanen M, Chotteau-Lelievre A, de Launoit Y, Isomaa V, Vainio S, et al. Ontogeny of 17beta-hydroxysteroid dehydrogenase type 2 mRNA expression in the developing mouse placenta and fetus. Mol Cell Endocrinol. 1997; 134: 33–40. [Medline] [CrossRef]

51. Mindnich R, Haller F, Halbach F, Moeller G, Hrabé de Angelis M, Adamski J. Androgen metabolism via 17beta-hydroxysteroid dehydrogenase type 3 in mammalian and non-mammalian vertebrates: comparison of the human and the zebrafish enzyme. J Mol Endocrinol. 2005; 35: 305–316. [Medline] [CrossRef]